Development of water surface mobile robot inspired by water striders

Kenji Suzuki[1] ✉, *Richard Waki Ichinose*[1], *Hideaki Takanobu*[1], *Hirofumi Miura*[2]

[1]*Department of Mechanical Engineering, Kogakuin University, 2665-1 Nakanomachi, Hachioji-shi 192-0015, Tokyo, Japan*
[2]*Kogakuin University, 1-24-2, Nishi-Shinjuku, Shinjuku, Tokyo 163-8677, Japan*
✉ *E-mail: ksuzuki@cc.kogakuin.ne.jp*

Published in Micro & Nano Letters; Received on 3rd March 2017; Revised on 30th May 2017; Accepted on 13th June 2017

This work describes a water surface mobile robot utilising surface tension forces. Recent biological studies on water striders revealed how they stay afloat and move on the surface of water. By using their hairy legs coated with hydrophobic substance produced, they increase the water repellency and float by the surface tension. This work focuses on understanding the static and dynamic interactions between supporting legs and the surface of water. First, microstructured wire legs were fabricated by using femtosecond laser machining to enhance the water repellency. Then the supporting force, the pull-off force and the drag force were measured to find the suitable legs for water strider robot. Finally, by assembling the legs optimised for supporting load and propulsion, a water strider robot weighing 4.39 g was developed. The robot successfully moved on the surface of water at a speed of 59.2 mm/s.

1. Introduction: Recently, there has been considerable interest in biologically inspired small mobile robots. When robots are scaled down to millimetre sizes, the surface tension force dominates the gravity force and the buoyancy. Therefore, we focused on water striders that use this scaling effect to stay afloat and move on water without breaking the water surface. The legs of water striders are covered by large numbers of tiny hairs, as shown in Fig. 1, and wax is secreted on the surface. These structural and chemical properties enhance the water repellency of the leg and the contact angle of water reaches 167° [1]. There have been many studies on biologically inspired water strider robots [2–13], and mechanisms of the water surface locomotion have been gradually clarified. However, the water repellency of supporting legs of these robots is still inferior to the insect water strider. In addition, optimal shape and structures of the legs for supporting weight and propulsion on the surface of water have not been clarified.

In this Letter, to obtain highly water-repellent legs for water strider robots, microgrooves were fabricated on the surface of a brass wire of 0.5 mm in diameter using femtosecond laser machining, and a water-repellent agent was coated on the wire. Then, we examined effects of the microgrooves on supporting, pull-off and drag forces on the water surface. Finally, a water strider robot with the hydrophobic legs was assembled and the performance on the surface of water was tested.

2. Fabrication of hydrophobic legs: To stay and move on the surface of water, highly water-repellent legs are required. In this Letter, we fabricated spiral grooves on the surface of brass wires of 0.5 mm in diameter using a femtosecond laser machining system (Cyber Laser Inc., IFRIT). The short-pulse laser was irradiated along the axis of the brass wire with a feed speed (FS) of 25 µm/s while the wire was rotated by using a stepping motor. By rotating clockwise (CW), a single-grooved wire (*Single*) was obtained, and by rotating clockwise and counterclockwise (CCW), a cross-grooved wire (*Cross*) was fabricated. These processes are shown in Fig. 2, and the conditions of the laser machining are shown in Table 1. An image of the single-grooved wire and a surface profile of the grooves obtained by a laser scanning microscope are shown in Fig. 3. After processing, the

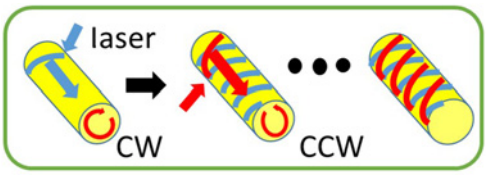


Fig. 2 *Fabrication process of grooved wires*

Table 1 Conditions of the process

	Single	Cross
laser power	100 mW	
wavelength	800 nm	
pulse width	180 fs	
FS	25 µm/sgg	
rotation	CW	CW and CCW
groove's depth	15 µm	18 µm at a cross-point
groove's pitch	48 µm	48 µm

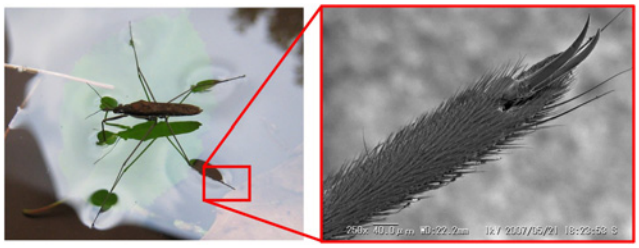


Fig. 1 *Scanning electron microscopy image of a water strider's leg*

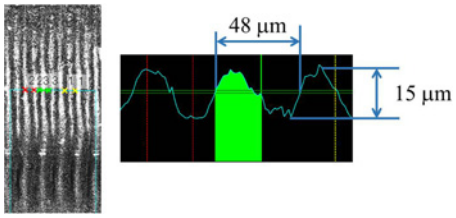


Fig. 3 *Image of the single-grooved wire and a surface profile of the grooves obtained by a laser scanning microscope*

© The Institution of Engineering and Technology 2017

Single and Cross wires were coated with a water-repellent agent, *FS-1010* (Fluoro Technology Company) by dipping to cover the microstructured surfaces. These wires were compared with an unprocessed and uncoated wire *(Brass)* and an unprocessed wire coated with *FS-1010* on measurements of forces.

3. Force measurements

3.1. Measurement of supporting force and pull-off force: To facilitate the experiment, the laser-machined wire legs were bent into the shape as shown in Fig. 4, and attached to a double cantilever spring. The wire leg was placed on the surface of water, which was moved vertically by a remote-controlled Z-stage. The experimental setup is shown in Fig. 5.

The principle of measuring, supporting and pull-off forces is shown in Fig. 6. To measure the supporting force, the leg was pressed on the water surface, which was lifted until the surface was broken by the leg. The supporting force was obtained by measuring the upward deflection of the spring by a laser displacement sensor. To measure the pull-off force, the leg was first pushing the water surface, and then the water surface was gradually moved down by the Z-stage until the leg was completely pulled-off. The pull-off force was obtained from the maximum downward deflection of the spring. Each measurement was performed three times and these data were averaged.

The experimental results of the supporting force are shown in Fig. 7. The Brass leg shows the lowest force, and the other legs, which are hydrophobic, have almost the same value of the supporting force.

The theory of surface tension force indicates that the maximum supporting force per unit length due to the surface tension is constant and equal to twice of the surface tension force of water γ, as shown in Fig. 6, if the contact angle is >90° [2, 5]. The experimental results agree with the theory.

The measurement results of pull-off force are shown in Fig. 8. The pull-off forces of the microgrooved legs are lower than those of the unprocessed ones. There is a tendency that the pull-off force decreases with increasing the water repellency of the leg surface.

3.2. Measurement of drag force: To design the legs suitable for supporting weight and propulsion, the drag force was measured by moving the legs horizontally on the surface of water. A low drag force is required for the supporting legs, whereas a high drag force is required for the actuating legs because a thrust force acts on the actuating legs as a reaction of a drag force. The experimental setup for measuring the drag force is shown in Fig. 9. The wire leg was fixed to the bottom of a double cantilever spring, pressed on the surface of water and moved horizontally by using a linear guide apparatus with changing the speed from 50 to 250 mm/s. The depth from the original water

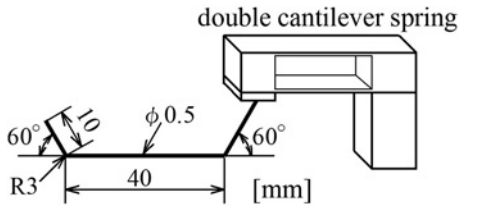


Fig. 4 *Dimensions of the wire leg*

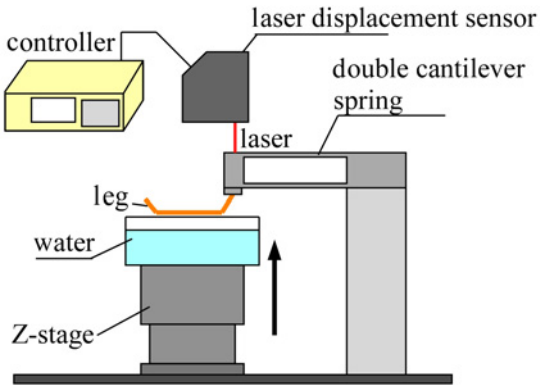


Fig. 5 *Measurement apparatus of supporting and pull-off forces*

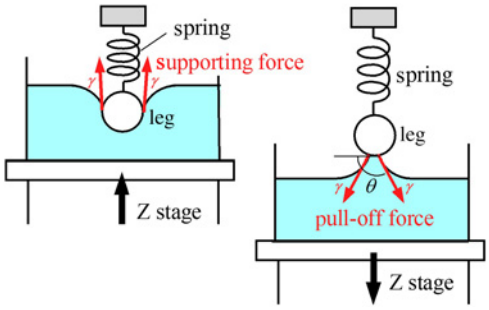
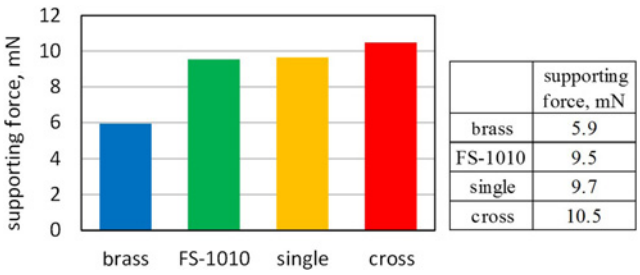
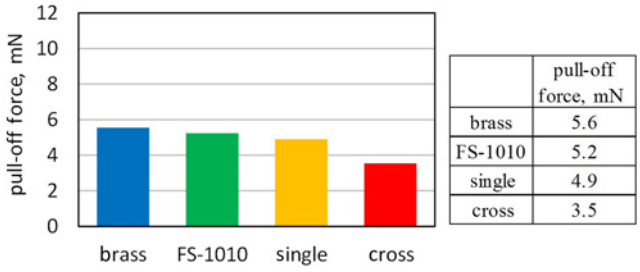


Fig. 6 *Principle of the measurements*



	supporting force, mN
brass	5.9
FS-1010	9.5
single	9.7
cross	10.5

Fig. 7 *Results of measurement of supporting force*



	pull-off force, mN
brass	5.6
FS-1010	5.2
single	4.9
cross	3.5

Fig. 8 *Results of measurement of pull-off force*

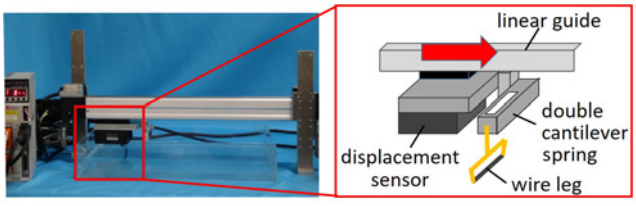


Fig. 9 *Measurement apparatus of drag force*

© The Institution of Engineering and Technology 2017

doi: 10.1049/mnl.2017.0134

surface can be varied with Z-stage from 0 to 4 mm. The drag force was obtained by averaging the deflection of the cantilever while the leg was moved at a constant speed.

The experimental results are shown in Figs. 10 and 11, and Table 2. At depths of 3 and 4 mm, the legs were all submerged and these data were omitted. The drag force increased with increasing velocity and depth when the leg was moved on the dimple of the water surface. However, when the wire is completely submerged, the drag force decreases significantly. By comparison between two graphs at different speeds in Fig. 10, and at different depths in Fig. 11, it is found that the microstructures on the surface (Single and Cross) make the legs hardly submerged, while they

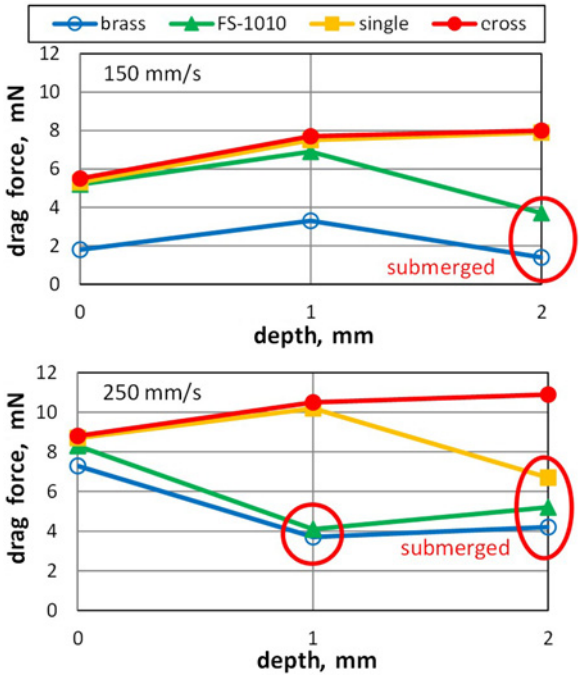


Fig. 10 *Relationship between drag force and depth*

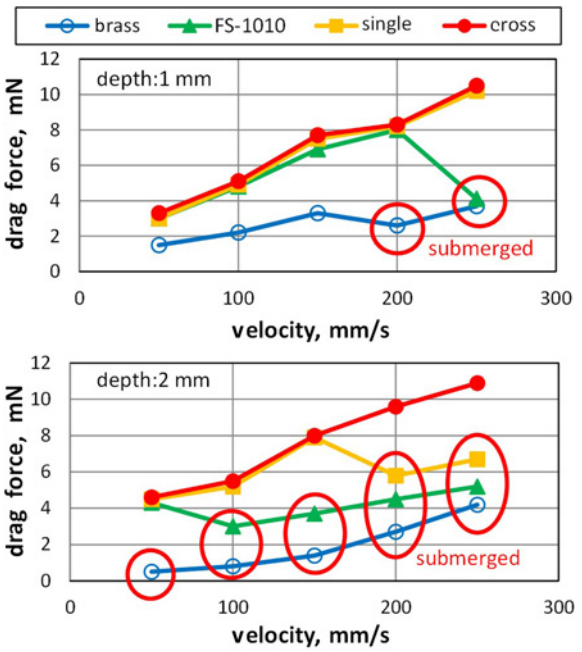


Fig. 11 *Relationship between drag force and velocity*

Table 2 Values of drag force per conditions

Brass	0 mm	1 mm	2 mm	FS-1010	0 mm	1 mm	2 mm
50 mm/s	0.7	1.5	0.2	50 mm/s	2.4	3.0	4.3
100 mm/s	1.0	2.2	0.8	100 mm/s	4.0	4.8	3.0
150 mm/s	1.8	3.3	1.4	150 mm/s	5.2	6.9	3.7
200 mm/s	3.0	2.6	2.7	200 mm/s	6.5	8.0	4.5
250 mm/s	7.3	3.7	4.2	250 mm/s	8.3	4.1	5.2

Single	0 mm	1 mm	2 mm	Cross	0 mm	1 mm	2 mm
50 mm/s	2.6	3.0	4.5	50 mm/s	3.1	3.3	4.6
100 mm/s	4.1	4.9	5.2	100 mm/s	4.3	5.1	5.5
150 mm/s	5.3	7.5	7.9	150 mm/s	5.5	7.7	80
200 mm/s	6.6	8.2	5.8	200 mm/s	6.7	8.3	9.6
250 mm/s	8.7	10.2	6.7	250 mm/s	8.8	10.5	10.9

do not affect the drag force. In Table 2, underlined figures indicate that the legs are submerged. The results show that the microstructured water-repellent legs are less submerged. The cross is an only leg which does not sink in all conditions in Table 2. Therefore, the cross is less submerged, that is, it has a higher 'dynamic' supporting force when it is moving on the water surface.

3.3. Relationship between the drag force and the shape: To optimise the shape of the supporting legs, relationship between the shape of the leg and the drag force was investigated. The supporting leg needs a high static and dynamic supporting force to prevent submerging, and a low drag force to move faster. We prepared legs with different shapes: a circle, a long ellipse, a trapezoid and a diamond. They are all made of a 100 mm long brass wire without grooves and sprayed with a fluorine-based water-repellent agent, HIREC1450NF (NTT Advanced Technologies), which includes microparticles and can easily make the surface uneven and hydrophobic. The contact angle of the sprayed surface is ~145°. The top views and dimensions of the wire legs are shown in Fig. 12. By using the same method as Section 3.2, we measured the drag force acting on each leg. The experimental results are shown in Fig. 13.

The circular leg has the highest drag force and the other legs, which have the same width of 15 mm, exhibit almost the same value of drag force. Previous studies [4, 12] showed that the drag force of a straight wire leg on the water surface is proportional to the projected area A of the convex and concave water surfaces, (see Fig. 14). The experimental results shown in Fig. 13 support this hypothesis. Supporting legs need to have a small width to reduce the drag force. In the cases of trapezoid- and the diamond-shaped legs, minute horizontal vibration was observed during the

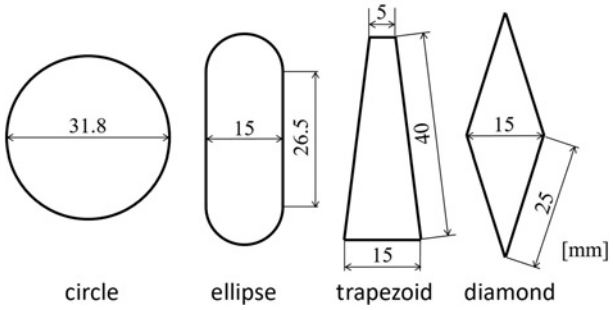


Fig. 12 *Top views and dimensions of wire legs with various shapes (L = 100 mm, ϕ=0.5 mm)*

© The Institution of Engineering and Technology 2017

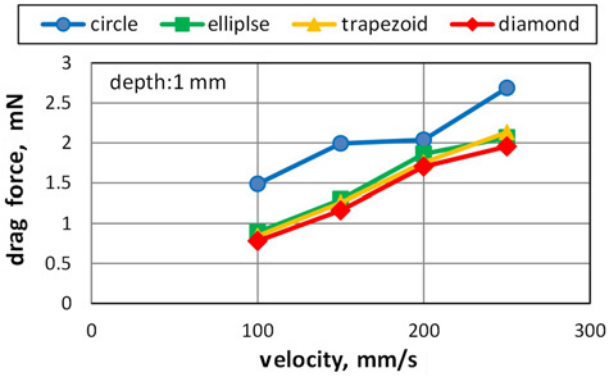


Fig. 13 *Effect of shape of the leg on the drag force*

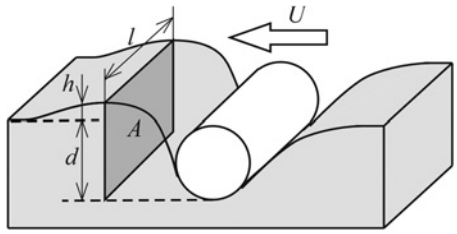


Fig. 14 *Projected area A of the convex and concave water surfaces*

movement on the surface of water. Therefore, the elliptical shape is more stable for the supporting legs.

4. Water strider robot: A six-legged water strider robot was designed on the basis of the experimental results. The fore and rear legs support the weight of the robot and the middle legs are driven for propulsion, which is in the same way as an insect water strider.

The supporting legs need a high supporting force and a low drag force. According to the results of experiments, a certain level of water repellency is enough to generate static supporting force, while high water repellency is necessary to generate a high dynamic supporting force while moving on the surface of water. Unprocessed brass wires sprayed with the water-repellent agent HIREC145NF were used for the supporting legs to obtain highly water-repellent legs easily. To reduce the drag force, elliptical wire legs with a circumferential length of 130 mm and a width of 10 mm were made. Total length of four supporting legs is 520 mm and they can support 100 mN (10.2 mg), which is approximately twice of the robot weight.

The actuating legs, which generate a thrust force as a reaction of the drag force, need a high drag force and a low pull-off force. According to the experimental results, a highly water-repellent leg shows a low pull-off force and hardly sinks even when it is driven fast on the water surface. To obtain a high thrust force, legs with large lateral width are required. We used a 40 mm long brass wire coated with HIREC145NF for the actuating leg, as shown in Fig. 15. Tip of the leg was bent upward to prevent breaking the water surface.

The actuating leg is attached to the tip of a four-bar link called 'Chebyshev-link mechanism' [13] as shown in Figs. 15 and 16. The mechanism is driven by a DC motor, and generates a D-shaped motion of the leg, as shown in Fig. 17. The leg is moved linearly above the water surface and returns quickly along the curved line on the surface of water.

A carbon material was used for the robot body to reduce the weight and each part is fabricated by femtosecond laser machining. Then, the robot body and the legs were assembled. A photograph of

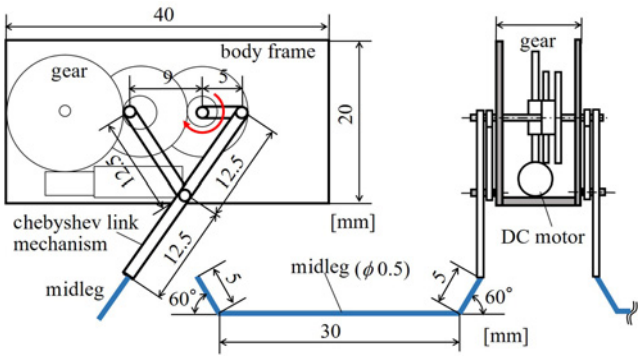


Fig. 15 *Driving mechanism of the actuating legs*

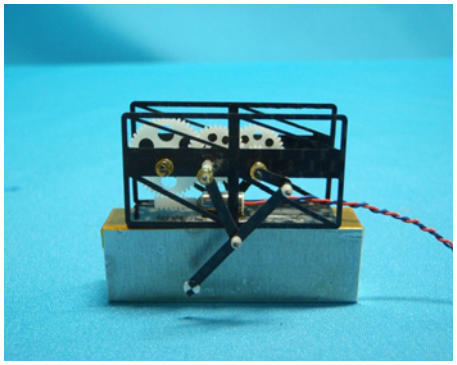


Fig. 16 *Photograph of the driving mechanism*

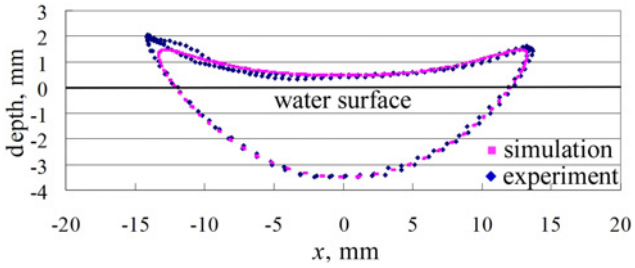


Fig. 17 *Trajectory of the tip of the driving mechanism*

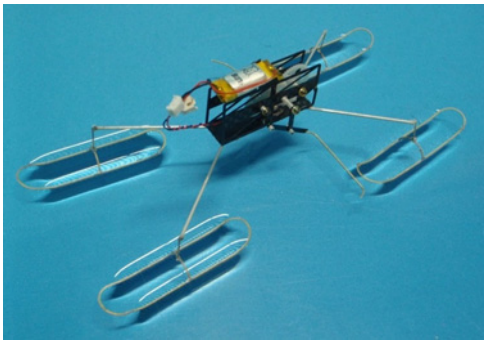


Fig. 18 *Water strider robot*

the robot is shown in Fig. 18. It weighs 4.39 g including a DC motor and a lithium-polymer battery.

Trajectory of the actuating leg measured with a high-speed camera is shown in Fig. 17. The measured trajectory agrees well with the calculated one. The robot successfully moved on the

© The Institution of Engineering and Technology 2017

doi: 10.1049/mnl.2017.0134

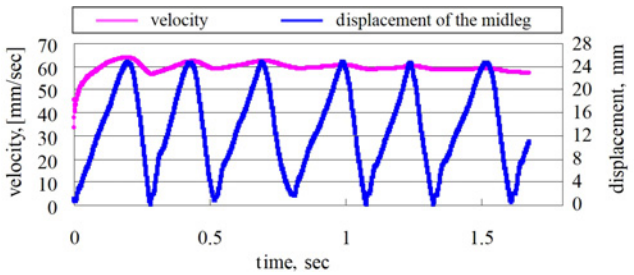


Fig. 19 *Velocity of the robot and displacement of the middle leg*

surface of water autonomously. Velocity of the robot and displacement of the middle leg obtained from images of a high-speed video camera are shown in Fig. 19. The maximum velocity of the robot was measured as 59.2 mm/s.

5. Conclusion: A brass wire, with a diameter of 0.5 mm was processed with a femtosecond laser to make spiral grooves, and coated with a water-repellent agent. The effects of microstructured surfaces on the supporting, pull-off and drag forces were investigated. The microstructured hydrophobic leg shows a low pull-off force and a high dynamic supporting force during the horizontal movement on the water surface. The experimental results show that the difference of microstructure does not affect the drag force and the elliptic shape for the supporting legs is the most stable to move on the water surface. A water strider robot with optimised legs was developed and it successfully moved on the surface of water at a speed of ∼60 mm/s.

6. Acknowledgments: This work was financially supported by the project-in-aid for the establishment of strategic research centers from the MEXT, Japan (Functional Microstructured Surfaces Research Center, in Kogakuin University).

7 References

[1] Gao X., Jiang L.: 'Water-repellent leg of water striders', *Nature*, 2004, **432**, p. 36

[2] Suzuki K., Koike H., Takanobu H, *ET AL.*: 'Study on water strider robot utilizing surface tension forces', *Trans. Jpn. Soc. Mech. Eng.*, 2009, **75**, (751), pp. 656–659, in Japanese

[3] Suzuki K., Takanobu H., Noya K., *ET AL.*: 'Water strider robots with microfabricated hydrophobic legs'. IEEE/RSJ Int. Conf. Intelligent Robots and Systems, San Diego, USA, October 2007, pp. 590–595

[4] Ozcan O., Wang H., Taylor J.D., *ET AL.*: 'Surface tension driven water strider robot using circular footpads'. 2010 IEEE Int. Conf. Robotics and Automation, Anchorage, USA, May 2010, pp. 3799–3804

[5] Song Y.S., Sitti M.: 'Surface-tension-driven biologically inspired water strider robots: theory and experiments', *IEEE Trans. Robot.*, 2007, **23**, (3), pp. 578–589

[6] Hu D.L., Prakash M., Chan B., *ET AL.*: 'Water walking devices', *Exp. Fluid Mech.*, 2007, **43**, pp. 769–778

[7] Zhang X., Zhao J., Zhu Q., *ET AL.*: 'Bioinspired aquatic microrobot capable of walking on water surface like a water strider', *Appl. Mater. Interfaces*, 2011, **3**, pp. 2630–2636

[8] Zhao J., Zhan X., Chen N., *ET AL.*: 'Why super-hydrophobicity is crucial for a water-jumping microrobot?', *Exp. Theor. Invest. Appl. Mater. Interfaces*, 2012, **4**, pp. 3706–3711

[9] Hu D.L., Chan B., Bush J.W.M.: 'The hydrodynamics of water strider locomotion', *Nature*, 2003, **424**, pp. 663–666

[10] Fujii S., Nakamura T.: 'Development of an amphibious hexapod robot based on a water strider'. Advances in Climbing and Walking Robots, Proc. Tenth Int. Conf., Singapore, July 2007, pp. 135–143

[11] Koh J.S., Yang E., Jung J.P., *ET AL.*: 'Jumping on water: surface tension-dominated jumping of water striders and robotic insects', *Science*, 2015, **349**, pp. 517–521

[12] Iwabe J., Suzuki K., Takanobu H., *ET AL.*: 'Biologically inspired water strider robot with microstructured hydrophobic legs'. Proc. Sixth Int. Symp. Aero Aqua Bio-mechanisms, Honolulu, USA, November 2014, pp. 246–249

[13] Tsukakoshi M., Suzuki K., Seki H., *ET AL.*: 'Water strider robot with microfabricated hydrophobic legs'. 2012 ASM-ISPS/JSME-IIP Joint Int. Conf. Micromechatronics for Information and Precision Equipment (MIPE2012), Santa Clara, USA, June 2012, pp. 306–308

© The Institution of Engineering and Technology 2017